Valorisation of banana peel waste as precursor material for different renewable energy systems

Johanna A. Serna-Jiménez[a,c,ϕ], Fernando Luna-Lama[b,ϕ], Álvaro Caballero[b], María de los Ángeles Martín[c], Arturo F. Chica[c], José Ángel Siles [c,*]

[a] Agricultural and Agro-Business Sciences Faculty, Universidad Tecnológica de Pereira, Carrera 27 10-02 Barrio Álamos. Edificio Nº 1A / Of: 117A, Pereira, Risaralda, Colombia.

[b] Department of Inorganic Chemistry and Chemical Engineering, Instituto Universitario de Nanoquímica (IUNAN), University of Cordoba. Campus Universitario de Rabanales, Ctra. N-IV, km 396, building Marie Curie (C-3). CP/14071 Cordoba, Spain.

[c] Department of Inorganic Chemistry and Chemical Engineering, University of Cordoba. Campus Universitario de Rabanales, Ctra. N-IV, km 396, building Marie Curie (C-3). CP/14071 Cordoba, Spain.

[*]Corresponding author: phone: +34 957218624; email: a92siloj@uco.es

[ϕ] J. Serna and F. Luna-Lama contributed equally to the work.

Abstract

Different valorisation processes of banana peel waste (BPW) were evaluated: combustion, production of activated carbon/batteries, and biomethanisation. This study showed that the combustion of BPW is an interesting option with a zero-carbon cycle. A mass balance demonstrated a low concentration of sulphurous compounds in the flue gases (0.01%, in volume), but the content of structural nitrogen dioxide was remarkable (0.35%). Additionally, BPW should be pre-dried to increase its lower calorific value (LCV) of 3000 kcal/kg. In contrast, mesophilic biomethanisation of BPW led to the generation of renewable methane (182 L_{STPCH4}/kg VS, volatile solids) and organic digestate, while its biodegradability was found to be 68%, under the study conditions. The obtention of porous activated carbon was also demonstrated employing a simple and low-cost method based on chemical activation/carbonisation of BPW with KOH porogen. The banana peel waste carbon obtained (BPW-C) showed low crystallinity,

[*] Corresponding author.
E-Mail addresses: andrea.serna@utp.edu.co (J.A. Serna-Jiménez), q12lulaf@uco.es (F. Luna-Lama), alvaro.caballero@uco.es (A. Caballero), iq2masam@uco.es (M.A. Martín), iq1chpea@uco.es (A.F. Chica), a92siloj@uco.es (J.A. Siles).

high purity and Brunauer-Emmett-Teller surface area (S_{BET}) of 264 m^2/g. BPW-C was tested as an anode electrode in lithium-ion batteries (LIBs) and a remarkable reversible capacity of 225 mAh/g at 0.2 C after 200 cycles was observed. These results indicate the feasibility of the carbonisation method of BPW to produce a highly demanded product in current society.

Keywords: Banana peel waste; biogas; activated carbon; lithium batteries.

1. Introduction

Current society is characterised by the generation of large volumes of agricultural and industrial residual biomass [1]. Banana peel waste (BPW) is the solid waste derived from processing banana and constitutes about 40% of fresh fruit weight. World banana and plantain (*Musa* spp.) production was estimated to be 155,220,025 tonnes in 2018 [2]. BPW is mainly generated in homes, restaurants, food outlets and the processing industry, the latter being the largest generator of such waste in a localised manner. These activities generate large amounts of putrefying waste, which in addition to not generating economic benefits to farmers or entrepreneurs, become a source of pollution, causing phytosanitary and environmental problems in the surrounding ecosystems. Although several management methods have been reported in literature, BPW are generally dumped in the production sites or landfilled and occasionally transformed into organic fertiliser or used for animal feed [3]. Nevertheless, Canto and Castillo [4] reported that the flour derived from *Musa* spp. waste used for animal feeding have low nutritional properties, leading to the necessity of including other supplements in dietsHaz clic o pulse aquí para escribir texto.. Other studies have demonstrated the possibility of using banana waste to obtain charcoal or paper. In addition, the effect of its antioxidant capacity in preventing carcinogenic diseases, Parkinson and Alzheimer

has also been reported [5,6]. However, despite the existing alternatives for the use of by-products and waste derived from banana cultivation, these are not usually applied at an industrial scale as they require significant economic investment and high energy demand. Consequently, the production of those commodities cannot be afforded in small banana processing plants [7]. Therefore, it is important to evaluate further sustainable alternatives to valorise BPW and meet current stringent regulations.

One of the most challenging problems for the whole world is climate change, and intensive efforts have been consistently made to reduce CO_2 emissions, ever since the Kyoto protocol and especially after the 2015 Paris Agreement [8]. Strategies for mitigating the effects of climate change include the use of renewable sources for generating energy. In this context, combustion of different residual fractions of *Musa* spp. cultivation (steam and leaves), either alone or making briquettes in mixtures with other substrates, has been reported to produce renewable fuel and minimise waste volume [7,9]. Rojas et al. [10] have recently evaluated BPW as raw material for energy generation and reported its average calorific value (16.12 MJ/kg) and ash content (9.92% dry basis), in comparison with other raw materials of biomass origin. Higher calorific value was obtained when BPW was pyrolysed (22 MJ/kg), although in terms of preliminary energy balance, more than 70% of the total energy output was attributed to the liquid pyrolytic products followed by the solid and gaseous products (aromatic, aldehyde, ketone and other functional groups) [11]. Thulu et al. [12] reported that the combustion characteristics of briquettes composed of BPW and saw dust competed favourably with firewood. Specifically, it was observed that the burning rate of briquettes varied within the range 2.4-2.5 g/min. But high levels of ash and deposit forming elements were detected from fuel pellets produced using agricultural residues

[13]. These facts have recently promoted the development of alternative revalorisation uses such as conversion of BPW into electricity using microbial fuel cell [14] or the integration of banana crop residues as biomass feedstock into conventional production of first-generation fuel ethanol from sugarcane [15]. However, energy requirements of biomass pretreatment steps are still a limiting factor for the industry.

Biomethanisation is a technically feasible and environmentally-friendly alternative within biotechnological applications. Anaerobic digestion of BPW generates renewable biogas and digestate, which may be applied in agricultural soils, with the consequent benefits for the *Musa* spp. manufacturing process [16,17]. Nevertheless, further studies are still required to optimise their feasibility and take real advantage of organic waste.

Another promising alternative for valorising BPW might be to convert it to activated carbon by simple and low-cost carbonisation methods through: physical (CO_2 and O_2) or chemical activation (H_3PO_4, KOH, $ZnCl_2$, etc.); which allow developing carbonaceous porous structures with large surface area. This textural property confers activated marked carbo versatility as adsorbent/trapping materials for wastewater treatment (removal of heavy metals, solvents, pesticides or dyes) or even as renewable energy storage sources [18]. For example, recent studies in energy storage systems (ESS) have put significant attention to the use of biomass-derived carbons for the development of lithium-ion batteries (LIBs) [19].

The generation of "green carbon" is advantageous because the production process from available natural biomass is simple, economical and environmentally friendly. At the same time, the final product has high porosity, tunable morphology, low bulk density and high thermal and chemical stability [20]. The production of carbon from waste biomass such as bamboo wood [21], lignin [22], loofah [23], seaweed [24], or rice husk

100 [25] has been reported in literature. In this context, chemical activation methods are
101 crucial to promote a carbonaceous structure of high porosity and large surface area, with
102 applicability as a sustainable anode for high-energy LIBs applications in electric
103 vehicles [26]. Specifically, different residual substrates have been used as precursors for
104 an activation/carbonisation process with KOH porogen to obtain an added value of
105 activated carbon. For example, Caballero et al. [27] obtained olive stone activated
106 carbon with a specific capacity of 170 mAh/g at 0.2 C, after 100 cycles in LIBs. The
107 suitable application of BPW-derived carbons for LIB has been reported by Stephan et
108 al. [28] using $ZnCl_2$ and KOH as activating agents. However, they needed a long and
109 complex synthesis process, including a 5-day activation stage, to obtain electrodes with
110 a drastic drop of specific capacity (921 to 217 mAh/g) in just 10 charge/discharge
111 cycles.
112 The main objective of this research is to evaluate the feasibility of three valorisation
113 alternatives for abundant BPW: (1) combustion (in-depth theoretical assessment of the
114 composition of flue gases and flame temperature); (2) biomethanization under
115 mesophilic conditions; (3) and production of activated carbon with applicability as the
116 anode in high-performance LIBs, through a simple, fast and environmentally-friendly
117 method. This innovative comparative study might be considered of special interest
118 within the frame of biorefinery and circular economy in the agri-food industry.
119 **2. Materials and Methods**
120 **2.1 Organic waste**
121 Banana peel waste was obtained from a banana plantation (*Banana paradisiaca*) located
122 in Colombia, one of the main producers of *Musa* spp. around the world. The chemical
123 composition of BPW is shown in Table 1.

2.2 Experimental set-up

2.2.1. Biomethanisation

The feasibility of anaerobic digestion of BPW was evaluated at laboratory scale using two continuous stirred-tank reactors (1 L) fed in semi-continuous mode. Four connections located at the top of each reactor allowed loading the residual substrate and samples withdrawal and ventilation of biogas and injection of nitrogen to favour the absence of oxygen. A thermostatic jacket containing hot water allowed maintaining mesophilic temperature inside the reactors (35 ºC). Boyle-Mariotte reservoirs (1 L) were used to measure methane generated by water displacement. A NaOH solution (6N) was added to tightly closed bubblers connected between each reactor and methane measuring device and used to remove carbon dioxide contained from biogas. Methanogenically-active granular sludge derived from an anaerobic digester used to valorise agro-industrial waste in the company EMACSA (Cordoba, Spain) was inoculated in each reactor (pH = 7.76 ± 0.02; VS = 9900 ± 110 mg/kg wet inoculum). The methanogenic activity of the inoculum was found to be 68 mL_{STP} CH_4/g COD (chemical oxygen demand)·h.

2.2.2. Activated carbon

The successive and high purity chemical reagents used for activated carbon synthesis were supplied by Panreac: sulfuric acid 96% and potassium hydroxide 85%.

2.2.3. Batteries

The successive and high purity chemical reagents used for electrode preparation were supplied by Fluka (Polyvinylidene fluoride, PVDF), Timcal (Carbon Black Super P), and Sigma-Aldrich (1-Methyl-2-Pyrrolidone anhydrous 99.5% and Lithium

147 hexafluorophosphate solution in ethylene carbonate and diethyl carbonate, 1.0 M $LiPF_6$
148 in EC/DEC (1:1; v/v), battery grade).

149 **2.3. Experimental procedure**

150 *2.3.1. Burning BPW*

151 The procedure to evaluate the feasibility of the controlled incineration of BPW in a
152 combustion chamber consisted of carrying out a mass balance to estimate the
153 concentration of the main gaseous compounds contained in the gaseous emissions (CO_2,
154 NO_x, SO_2, H_2O, N_2 and O_2) [29]. The combustion of the different components of BPW
155 under study was assumed to be complete. In addition, the air excess in relation with the
156 theoretical value required in the oxidation reactions taking place was fixed at 40%. That
157 value of air excess would allow a concentration of oxygen in the flue gas as high as 6%
158 (d.b.) according to the Spanish Royal Decree 687/2011 of 13 May, which amends Royal
159 Decree 430/2004 of 12 March establishing new rules on the limitation of emissions into
160 the atmosphere of certain pollutants from large combustion plants, and fixing certain
161 conditions for the control of emissions into the atmosphere of oil refineries [30].
162 An additional energy balance (EB) was performed to estimate the production of thermal
163 nitrogen oxides (NO_x) and flame temperature (T), under the next conservative
164 assumptions: (1) incineration was carried out under adiabatic conditions and flue gas
165 absorbed the heat generated totally; (2) the flowrates of SO_2 and NO_x were not
166 significant; and (3) the reference temperature was fixed at 25 ºC. Eq. 1 shows the
167 equation of the EB: $m_{BPW} \cdot LCV = \sum \int_{25+273}^{T} m_i \cdot Cp_i \cdot dT$ (Eq. 1), where m_{BPW} is equal
168 to 1 kg BPW (calculation basis), LCV is the lower calorific value (kcal/kg), Cp_i is the
169 heat capacity of N_2, O_2, H_2O and CO_2 (kcal/kg·ºC), and T is the flame temperature (ºC).
170 The following equation allowed the calculation of the lower calorific value of BPW:

$LCV = HCV - (m_{H_2O}/m_{BPW}) \cdot \lambda$ (Eq. 2), where *HCV* is the higher calorific value (kcal/kg), m_{H_2O} represents kg of H_2O contained in the substrate and water generated after burning H_2, and λ, expressed as kcal/kg, represents the latent heat of water vaporisation using a reference temperature of 25 ºC. The calculation of *Cp* for N_2, O_2, H_2O and CO_2 was carried out by equation (3): $Cpi = a + bT + cT^2$ (Eq. 3), where *a*, *b* and *c* corresponds to parameters for gaseous N_2, O_2, H_2O and CO_2 [31]. The mass and energy balances were solved by Mathcad software ® (version 14).

2.3.2. Biomethanisation

BPW was chopped and homogenised through blending (particle diameter lower than 2 mm). Subsequently, BPW was dried at 60 ºC for 24 hours and fed into the anaerobic reactors. The bioreactors were previously loaded with anaerobic sludge as inoculum (7 g VS/L, which was activated and acclimatised before carrying out the experiments with BPW. A synthetic solution composed of lactic acid, sodium acetate and glucose (GAL solution) at concentrations of 20.8 mL/L, 25 g/L and 50 g/L, respectively, was fed in the reactors to activate the inoculum. The GAL load fed into the reactors during the activation period was increased from 0.25 to 1.00 g VS/L for 21 days. Subsequently, and to acclimatise the inoculum/BPW, the reactors were fed with several loads of 1.00 g VS/L, where BPW and GAL were mixed at increasing ratios (BPW/GAL: 0.25/0.75; 0.50/0.50; 0.75/0.25; 1.00/0.00, respectively). The production of biogas with each load lasted a maximum time of 48 h. Once the acclimatisation process finished, BPW was load in the reactors as sole substrate at increasing concentrations from 0.5 to 1.0, 1.5, 2.0. 2.5, 3.0, 3.5 and 4.0 g VS/L (each load was carried out at least in duplicate). The maximum time required for complete biomethanisation of each load was 50 h. The volume of methane was regularly quantified by water displacement, and samples were

195 withdrawn before each load was fed. The solid fraction of samples was recirculated into
196 de digesters after centrifugation at 2000 pm. The duration of the experimentation
197 (acclimatisation and biomethanisation of BPW) lasted 60 days.

198 *2.3.3. Activated carbon*

199 The preparation of BPW activated carbon (BPW-C) was carried out through a simple
200 and sustainable method. Firstly, banana peels were cut into small pieces (20-30 mm)
201 and washed with 5% (v/v) H_2SO_4 diluted solution under stirring at 25 ºC for 3 h. Then,
202 the BPW was washed with distilled water until neutral pH and subsequently dried at
203 120 ºC for 12 h. The dried residues were grinded in a ball mill (Retsch PM100,
204 Germany) at 300 rpm for 30 min (a reaction recipient of 125 mL and 8 stainless steel
205 balls (10 mm diameter) were used). Subsequently, the homogenised powder was
206 impregnated with a KOH porogen solution at a BPW (dried):KOH mass ratio of 1:1 and
207 maintained under stirring and heating at 85 ºC for 3 h, until a solid paste was obtained.
208 Such solid phase was dried (120 ºC, 12 h). Finally, the impregnated product was heated
209 in a quartz tubular oven up to 700 °C (10 ºC/min) and held under N_2 atmosphere (50
210 mL/min) for 1 h to obtain activated carbon. After carbonisation, filtration and washing
211 of carbon with distilled water was carried out until neutral pH was reached to remove
212 the porogen and remnant traces of impurities.

213 *2.3.4. Batteries*

214 Preparation of electrodes for LIBs was carried out through mixing BPW-C with PVDF
215 binder and carbon black Super P conductive agent (80:10:10, respectively), in 1-methyl-
216 2-pyrrolidinone (NMP) solvent. Coating onto cupper foil (9 μm thickness) of the
217 obtained slurry was carried out using the "doctor blade" technique (25 μm thickness).
218 Finally, the electrodes were cut (13 mm diameter disks) and dried in a glass oven

(Büchi, Germany, 120 °C, 12 h), until cell assembling. The active material loading in all anode electrodes prepared for electrochemical tests was 1 mg/cm^2.

Cells assembling was performed on coin cells CR2032 model inside an argon-filled glove box (M-Braun 150 model; $H_2O \leq 1$ ppm) using a lithium metal disk as counter and reference electrodes (13 mm diameter). A volume of 30 μL of $LiPF_6$ was added per anode in EC:DEC (50:50; v/v) commercial electrolyte. The electrochemical cycling tests were performed on a battery tester system (model Arbin BT2143, USA) within a voltage range of 0.01–3.00 V. A constant current of 0.2 C (74.4 mA/g) was used for the discharge/charge tests (considering the theoretical capacity of graphite 1C: 372 mA/g). Different current densities every 10 cycles (0.1C, 0.2C, 0.5C, 0.8C, 1C, 2C and return to 0.1C) were fixed for rate capability tests. Cycling voltammetry (CV) was recorded in a potenciostat Pgstat204 (Metrohm, Switzerland) at 0.1 mV/s between 0–3V.

2.4. Physico-chemical analytical methods

The following variables were analysed to characterise BPW: moisture (%), mineral solids (MS, %), volatile solids (VS, %), total solids (TS, %), phosphorus content (P-P_2O_5, %), metals (mg/kg), elementary analysis (%) and higher calorific value (HCV, kcal/kg). Total soluble organic carbon (TOC, mg/kg), total soluble carbon (TC, mg/kg), inorganic soluble carbon (IC, mg/kg), pH, conductivity (μS/cm) and short-chain volatile organic acids (mg/kg), were measured in aqueous extract (1:25 ratio), according to the US Department of Agriculture and the US Composting Council [32]. Atomic absorbance spectrophotometry was used to quantify metal content in a A-Analyst 300 analyser (Perkin Elmer, UK). The profile of volatile fatty acids (C_2-C_6) was analysed by gas chromatography (HP 5890, USA). The HCV of BPW was quantified by Calorimetry (Parr 6300, USA), while elementary analysis (BPW and BPW-C) was

243 carried out using an analyser LECO CHN-1000 and LECO S632 (USA). An infrared
244 spectrometer Shimadzu TOC-VCSH (Japan) was used to determine TOC, TC and IC.
245 The effluent of the anaerobic reactors was characterised after each load by analysing the
246 following parameters: pH, conductivity (μS/cm), solids (%), short-chain organic acids
247 (mg/kg), alkalinity (Alk, mg $CaCO_3$/L), concentration of total soluble nitrogen (TSN,
248 mg/g), and soluble phosphorus (P_2O_5, %), in according to the Standard Methods of the
249 American Public Health Association [33]. A TOC-V CSH/CSN total organic carbon
250 analyser was used to quantify the concentration of TSN.
251 The structure of activated carbon was analysed by X-Ray Diffraction (XRD) (Bruker
252 D8 Discover USA diffractometer). The system generates monochromatic Cu K_α
253 radiation (λ = 1.5406 Å). The diffractogram was recorded between 10–80 º (2θ) with a
254 step size of 0.02 ° and 0.2 s per step. Thermogravimetric analysis (TGA) was used to
255 determine weight loss in different atmospheres (oxygen and nitrogen, flux 100 mL/min)
256 heating up from 30 to 800 ºC at 10 ºC/min (Mettler Toledo-TGA/DSC, USA). The
257 Brunauer–Emmett–Teller (BET) surface area was obtained from N_2 adsorption-
258 desorption isotherms at a temperature of liquid nitrogen (77 K) (Micromeritics ASAP
259 2020, USA). The density functional theory (DFT) was used to calculate pore size
260 distribution.

261 **3. Results and discussion**

262 **3.1. Controlled incineration of BPW**

263 An alternative solution to the inconveniences associated with agro-industrial disposal
264 might be biomass fuel for generating power. Waste incineration is commonly carried
265 out, especially in those countries where waste-related policies regulate waste disposal
266 on landfill [34]. The process consists of generating heat and simultaneous removal of

267 pathogenic biomass waste under a complete oxidative and controlled combustion
268 carried out in an engineered device. Industrially, thermal energy generated in the
269 furnace is transferred to boilers to produce hot and pressurised water steam and
270 electricity after turning a turbine connected to an alternator [35]. The elementary
271 analysis and BPW moisture are shown in Table 1. According to the elemental analysis
272 of the waste at different times during the production period, the LCV of BPW was
273 found to be 3000 kcal/kg (once the peels were dried, maintaining the moisture content
274 of 20%, in accordance with ISO/DIS 17225-1:2020).
275 Consequently, combustion of BPW might be an interesting alternative to valorise BPW
276 to generate heat and electricity. As described in the Materials and Methods section, a
277 mass balance was carried out to estimate the theoretical composition of the flue gases
278 generated by burning BPW. The concentration of different compounds in the emitted
279 flue gases, expressed as a percentage in volume, was 12.14% CO_2, 0.01% SO_2, 0.35 %
280 NO_2, 14.07 % H_2O, 5.18% O_2 and 68.25% N_2.
281 It is worth noting that the concentration of sulphur dioxide (SO_2) was found to be 208
282 mg SO_2/m^3_{STP} (d.b.; STP: 1 atm and 0ºC). Such figure does not exceed the limit for 50-
283 100 MW biomass plants (400 mg SO_2/m^3_{STP}), as established under Spanish Royal
284 Decree 687/2011 [30]. This is a remarkable benefit of controlled BPW incineration,
285 especially in comparison with burning coal or coke, which frequently lead to the
286 emission of highly polluted and dangerous gaseous streams. In contrast, the
287 concentration of structural NOx derived from the combustion of BPW might exceed the
288 limit indicated in such Royal Decree or by the Colombian resolution number 909/2008
289 [30,36], with Colombia being one of the main producers of *Musa* spp. Thermal NOx is
290 also generated from the air at high temperatures (> 1250-1300 ºC) [37]. The generation

291 of thermal NOx was estimated after calculating the theoretical flame temperature
292 reached by burning BPW, under the most unfavourable assumptions. After carrying out
293 the EB, the estimation of such theoretical temperature reached a value of 1488 ºC,
294 which is close to the limit reported by De Nevers (2017) [37]. Consequently, no
295 significant generation of thermal NOx would take place under the study conditions (9
296 mg/Nm^3 after 5 s of burning partially dried BPW powder). Although controlled
297 incineration of dried BPW might need the removal of structural NOx from the flue
298 gasses to comply with the air quality regulations, the reduced generation of thermal
299 NOx is a significant advantage to be considered. In contrast, it is worth noting that open
300 and uncontrolled combustion of residual substrates is not advisable due to the
301 generation of furans and dioxins and furans that may lead to air pollution [34]. Similar
302 studies reported low concentrations of NOx and SO_2 released during the combustion of
303 briquettes made of semi-dried banana leaves due to the low concentration of sulphur
304 and nitrogen and high levels of cellulose found in such part of the plant [38].
305 Nevertheless, direct thermal conversion might not be advisable if the moisture content
306 in the substrate is markedly high, which entails a low energy yield. The high moisture
307 content of BPW would make necessary simultaneous injection of another fuel to
308 promote the incineration process. Therefore, direct incineration of BPW could be
309 favourable in terms of net energy balance only when the previous drying had been
310 carried out [7].

311 **3.2. Anaerobic digestion of BPW**

312 *3.2.1. Reactors stability*

313 Biochemical conversion technologies are more favoured for wet substrates and more
314 eco-friendly. In this context, biomethanisation might be considered as one of the most

315 feasible valorisation technologies. Therefore, biomethanisation of BPW was evaluated
316 because this process allows the generation of renewable methane and recycling nutrients
317 contained in the digestate into agricultural soils. Figure 1A shows the evolution of pH
318 and the concentration of acetic, propionic, iso-butiric and iso-valeric acids, which were
319 the most abundant acids contained in the bioreactors, with the load added. The pH
320 values were virtually constant until the load of 2.5 g VS/L (7.74 ± 0.14) and within the
321 optimal range for stable biomethanisation [39,40].
322 Concerning the buffering capacity, favourable total alkalinity levels were detected
323 during the experimentation (2835 ± 130 mg $CaCO_3$/L). This buffering protects against
324 possible acidification of the reactors, which could be caused by different operational
325 conditions [41,42]. However, although the process was stable in terms of pH, a
326 decrease in this variable was observed at the highest BPW loads. This variation might
327 be a consequence of the increase in the concentration of acidity in the reactors
328 throughout the experimental process. As shown in Figure 1B, the concentration of
329 acetic acid increased from 48 ± 1 mg/L to 164 ± 4 mg/L, while propionic acid varied
330 from 11 ± 2 mg/L to 361 ± 14 mg/L.
331 On the other hand, the concentration of minority acids such as iso-butyric and iso-
332 valeric acids remained virtually constant at lower values than 40 mg/L and 14 mg/L,
333 respectively. In addition to the high concentration of acetic and propionic acids, the
334 variation in the ratio between their concentration (Propionic acid (eq)/Acetic acid(eq))
335 indicates the adequate functioning of the bioreactors. Hill and Bolte [43] reported that
336 an imminent signal of failure of an anaerobic digester occurs when this ratio reaches a
337 value higher than 1.40Haz clic o pulse aquí para escribir texto.. Under the operational
338 conditions tested, the ratio between acids varied within the range 0.18 - 1.79, exceeding

339 the limit as mentioned above from the load of 2.5 g VS/L, which indicates the beginning
340 of the destabilisation of the process at higher loads.
341 *3.2.2. Biodegradability and methane yield*
342 In the context of fermentation processes, it is known that waste from the food industry
343 and the agro-industrial and domestic sector can be exploited through biomethanisation
344 without drying the residual substrate. The production of renewable and highly energetic
345 methane is especially interesting when this derives from residual organic substrates. The
346 relation of the maximum methane volume produced (G_T) with each organic load added
347 to the reactors allowed the calculation of the mean methane yield from BPW. As shown
348 in Figure 1C, the methane yield derived from BPW was found to be 182 mL CH_{4STP}/g
349 VS. This result is in line with the methane yield reported by Bardiya et al. [44]. The
350 authors achieved a methane yield of 190 mL/g TS, but they inoculated 2-L anaerobic
351 digesters with a cattle dung digester sludge. A higher yield was obtained when banana
352 peel was dried and powdered (201 mL/g TS). In contrast, Jesuyemi et al. [45] obtained a
353 BMP of 17.14 L CH_4/kg VS employing two-phase digestion at 55 and 35ºC with loads
354 of 1, 1.5 and 2% TSHaz clic o pulse aquí para escribir texto.. However, the volatile fatty
355 acid profile increased with the 2% load, making the process unfeasible at higher loads
356 under the operational conditions tested due to the decrease in pH values. Other recent
357 studies, such as Joute et al., 2016 [46] and Barua et al, 2019 [47] reported methane
358 yields as high as 316 mL CH_{4STP}/g VS and 296 mL CH_{4STP}/g VS, respectively. The
359 difference in the yields obtained might find an explanation in the fact that different
360 concentrations of some inhibitory substances for biomethanization could be contained
361 in the digested substrates: tannins or organic acids [49-51]. In addition, different
362 anaerobic reactors configurations were used (including a bio-chemical methane

363 potential test), as well as co-digestion with other substrates (cow manure and water
364 hyacinth) and/or complex thermal pretreatments were applied, which also conditions the
365 efficiency of the process in terms of microbial activity.
366 With regard to biodegradability of BPW, this was calculated by a mass balance applied
367 to volatile solids added to the digesters and the remnant concentration in the digestate
368 after each load. A biodegradability rate of 68% was achieved under the study
369 conditions, which is lower than the value reported by Joute et al. [46], who codigested
370 banana peel waste with cow manure. This procedure might improve the availability of
371 nutrients for the microorganisms, the ratio among them and the dilution of inhibitory
372 substances.
373 According to the results obtained, the biomethanisation of BPW at mesophilic
374 temperature might be an interesting alternative to transform such polluting waste into
375 renewable fuel and electricity to be used in situ or even sold [52]. In addition, this
376 valorisation process reduces air pollution and do not contribute to global warming since
377 renewable biogas produced has a zero-carbon cycle. Higher transformation yields could
378 be achieved by applying different pretreatments to BPW (microbial, thermal, acidic-
379 alkaline, etc.) to increase biodegradability, with the consequent energy requirement. As
380 an alternative, digestate might be used as an organic amendment in agricultural soils due
381 to its high content in nutrients [7,53].
382 *3.2.3. Nutrients: Nitrogen and phosphorus*
383 Monitoring total soluble nitrogen in the mixing liquor of the digesters is essential to
384 evaluate the feasibility of subjecting BPW to biomethanisation. At particular
385 concentrations and chemical forms, soluble nitrogen is considered an important nutrient
386 for anaerobic microorganisms. However, it can also be an inhibitor at high

387 concentrations or unbalanced ratios with other substances. For example, at alkaline pH,
388 ammonium ions form free ammonia, one of the main inhibitors of anaerobic digestion
389 [49]. In contrast, some soluble forms of nitrogen are vital for anaerobic microorganisms,
390 especially to synthesise diverse types of essential biomolecules. Figure 2A shows the
391 variation in the concentration of total soluble nitrogen in the reactors throughout the
392 experimentation. The concentration of such a nutrient increased with the load added to
393 the reactors from 58.1 ± 0.1 to 840.0 ± 30.0 mg/kg. This fact is a consequence of the
394 remarkable concentration of nitrogen contained in BPW (Table 1). Although, depending
395 on pH and temperature conditions, a small fraction of such element might leave the
396 reactors with the biogas (in the form of traces of ammonia), soluble nitrogen usually
397 remains in the mixing liquor of the reactors [48]. These results align with the adequate
398 range reported by Chen et al. [49]. However, the literature on the appropriate nitrogen
399 concentration for anaerobic digestion is markedly variable and even contradictory,
400 depending on the substrate treated, type of reactor, operational conditions, etc.
401 With regard to phosphorus, this nutrient is essential for microorganisms involved in
402 biomethanisation processes, in combination with nitrogen and carbon [54]. However, as
403 shown in Figure 2B, a significant decrease in phosphorus concentration occurred at the
404 highest loads, probably due to microbial consumption and/or adsorption/precipitation
405 processes taking place in the mixing liqueur of the digesters. The fact that the variation
406 in phosphorus concentration is opposite to that observed in soluble nitrogen might be a
407 consequence of the high $N:P_2O_5$ ratio in BPW (9.13:1.00). Furthermore, the
408 requirements of both nutrients by the microorganisms are different, which also
409 conditions their availability in the reaction medium [55]. Consequently, the addition of
410 soluble phosphorus might be required for proper anaerobic digestion of BPW. An

interesting alternative to solve such an inconvenience and increase the process efficiency might be co-digesting BPW with another agroindustrial waste generated simultaneously in the same location. However, in comparison with the combustion of BPW, the kinetics of biomethanisation is markedly lower, and this fact could also undermine the applicability of the biotechnological process [56].

3.3. Activated carbon

3.3.1. Banana peels activated carbon: Structural characterisation

Figure 3A shows XRD diffractogram of BPW-C carbon. Two wide peaks are depicted at 23 º and 43 º that correspond to the (002) and (100) reflections planes of graphite (Pattern Diffraction File database, PDF 41-1487), respectively. Specifically, the weak (100) reflection determines the hexagonal arrangement structure by carbon atoms forming graphene layers, while the intense (002) reflection indicates a parallel stacking of those graphene sheets [57]. Both peaks confirm a disordered and amorphous carbonaceous structure, typical of biomass lignocellulosic carbons [27]. Figure 3B shows TGA measures recorded in N_2 and O_2. This information is essential to investigate the thermal stability and purity of this BPW-C material under both gaseous compounds. Firstly, TGA curve recorded under nitrogen atmosphere shows an initial weight loss of 8 % related to the water elimination in the porous carbon structure until 150 ºC, and immediately after a considerable second loss weight of 29 % appears from 150 ºC to 500 ºC. This result suggests the decomposition of external functional groups from the activated carbon. TGA curve in the presence of oxygen shows a similar weight loss between 100–150 ºC due to the water content. The second loss of weight occurs within the temperature range of 350–700 ºC, accounting for a significant percentage (82 %) associated with the complete combustion of carbon in the air. It is worth noting that

435 only a small fraction of porogen residues and natural ash content from banana peels
436 (14%) remained, reflecting an activated carbon of remarkable purity.

437 To quantify the purity of BPW-C, elemental carbon and nitrogen analyses were carried
438 out. As shown in Table 1, the concentration of carbon exceeds 80%, which is in line
439 with the weight loss observed in TGA in the presence of O_2. This high percentage of
440 carbon ratifies the formation of an optimal carbonaceous structure during pyrolysis.
441 Regarding nitrogen content, this is also considerable in BPW-C carbon, with a
442 percentage over 1%. It should be noted that the presence of nitrogen together with
443 oxygen in the carbonaceous structures are beneficial, as they contribute to the formation
444 of acid and basic functional groups, respectively. These superficial groups serve as
445 active sites to transport and store lithium ions into the carbon [58].

446 The study of the textural properties of BPW-C was carried out to determine porosity
447 structure and surface area. The N_2 adsorption-desorption isotherm plotted in figure 3C
448 shows a mixed shape type I/IV indicating: (1) the coexistence of micropores at low
449 relative pressures ($P/P_0 < 0.4$). (2) mesopores with a hysteresis loop (type H4) in high
450 relative pressure ($P/P_0 = 0.4–1$). According to the isotherm shape, BPW-C presents a
451 slit-shaped pores disposition with a high proportion of micropores and low content of
452 mesopores [59]. Table 1 also shows the BET surface area extracted from the isotherm,
453 pore volume and pore size values. BPW-C material exhibited a significant surface area
454 of 264 m^2/g, given principally by adsorption in micropores generated by an effective
455 activation with KOH porogen.

456 Figure 3D depicts the distribution of pore size applying the non-local density functional
457 theory (NLDFT) model [60], which allows pore volume and size data to be obtained.
458 According to the DFT pore distribution, BPW-C presents a major concentration of

micropores of 1–2 nm, and a minor proportion of mesopores (3–10 nm). The pore volume obtained is higher than 0.15 cm^3/g, mainly accumulated in micropores and contrasted with a mean value of pore size of 2.39 nm closer to the micropores region. Thus, the chemical activation of BPW with KOH porogen allowed the development of a porous and functionalised activated carbon with a large surface area and hierarchical porosity. The optimal distribution effectively provides different cavities for the diffusion/adsorption of lithium ions on the carbon structure [61].

3.4. Lithium-ion battery tests

The electrochemical performance of BPW-C as anode electrode in lithium-ion batteries was studied. The CV curves for BPW-C under a scan rate of 0.1 mV/s within the range 0-3 V are represented in Figure 4A. The voltammetry curves show the typical shape of non-graphitic carbons. A weak reduction peak appears at 0.67 V in the first cycle, associated with the electrolyte surface decomposition and subsequent irreversible formation of the solid electrolyte interphase (SEI) layer [62]. Furthermore, a high reduction peak ascribed to the intercalation of lithium ions within the carbonaceous structure appears near to 0 V. The opposite deintercalation process outside the carbonaceous structure is given by a weak oxidation peak between 0-0.5 V [63]. It should be noted that all peaks are less intense in the second and third cycles. In contrast, both cycles overlap, which indicates high reversibility during the insertion/extractions of lithium ions [64].

Figure 4B depicts the galvanostatic charge-discharge profiles for BPW-C anode at different cycles under a current rate of 0.2 C (74.4 mA/g) and voltage range between 0.01-3 V.

The electrode released capacity of 763 mAh/g in the first discharge cycle, showing an extended plateau between 0.5–0.8 V, concordance with the cathodic peak found at 0.7 V in the first CV curve. In contrast, the charge curve released a capacity value of 222 mAh/g and led to a low figure (30%) for coulombic efficiency (CE). This marked difference might be a consequence of two typical phenomena in disordered carbons: (1) the irreversible insertion of lithium ions into special positions (defects) of the porous carbonaceous structure [65]; and (2) the SEI membrane formation on the carbon surface [66]. In the second and further cycles, the discharge and charge branches exhibited lower capacity values because of the initial irreversibility, although both discharge and charge curves are nearly overlapped with each other (reaching a CE value close to 98%). This fact indicates the good electrochemical reversibility between discharge and charge reactions of BPW-C and the full SEI film stabilisation achieved by the porous carbonaceous structure under study [67]. BPW-C electrode delivered 225 mAh/g of reversible capacity after 200 cycles, and before the 100^{th} cycle, a marked increase in the specific capacity compared to the initial cycles was observed. The presence of significant pores provides active sites to insert additional lithium ions, increasing the transfer kinetics during the insertion/extraction processes in LIBs [68]. Thus, this added value material exhibits a notable reversible capacity and significant retention capacity with cycling. Figure 5A depicts the rate capability curves for BPW-C carbon electrode when the current rate was increased every 10 cycles from 0.1C to 0.2 C, 0.5 C, 0.8 C, 1.0 C and 2.0C, and then decreased to 0.1 C. According to these curves, BPW-C anode exhibited reversible stable capacities of 280, 237, 178, 136, 116 and104 mAh/g at the current densities of 0.1C, 0.2 C, 0.5 C, 0.8 C, 1.0 C to 2.0 C, respectively. Finally, the electrode supplied a reversible stable capacity of 230 mAh/g when the current density

turned back to 0.1 C again, which demonstrates the good capacity recovery for this material after suffering cycling at high current rates. Logically, the electrode presents a capacity fading, specially in the first cycles at low current rates, which might be due to the high cell polarisation at these rates [69]. In addition, it is worth noting that there is remarkable variation in the capacity values between charge and discharge branches at low current rates due to the irreversible intercalation of lithium ions into defects of the disordered carbon [70].

In general, BPW-C material present a good rate performance with high reversibility for the charge-discharge reactions and remarkable retention capacity at different current rates. The comparison of the specific capacity delivered for BPW-C with other electrodes at different current rates is plotted in Figure 5B. The high-performance rate exhibited by this material is better than other biomass-derived carbons reported in literature, some of which involve complex or unsustainable synthesis procedures [21-25]Haz clic o pulse aquí para escribir texto.Haz clic o pulse aquí para escribir texto.Haz clic o pulse aquí para escribir texto.Haz clic o pulse aquí para escribir texto.. Likewise, the performance of the BPW-C demonstrated in this work is clearly superior to that previously reported for banana fiber-derived carbon, where only a low-performance is observed when this residue is used as a source of porous carbon for LIB, showing only 10 charge/discharge cycles.Therefore, the possibility of valorising BPW as a porous carbon source for sustainable energy storage systems is demonstrated in this work.

4. Conclusions

Different environmentally-friendly processes to deal with BPW have been evaluated. Mesophilic biomethanisation of renewable BPW might be especially promising within the frame of circular economy as easily burnable methane can be obtained. Although

direct combustion of BPW also produces renewable energy, it has important drawbacks, especially at high moisture contents in the substrate. In contrast, preparation of a functional activated carbon for lithium storage in batteries is a markedly promising valorisation option. An easy and eco-friendly procedure based on chemical activation and carbonisation has been carried out. BPW-C carbon with suitable porosity has been demonstrated to be an adequate anode for LIBs. Comparatively, the carbonisation method might be considered as the most favourable alternative as this allows the transformation of BPW into a highly valued and demanded application currently, where significant amounts of carbon are required as a negative electrode. In general terms, the battery industry might absorb such waste and create a high-value market. Nevertheless, the type of exploitation to be implemented is highly dependent on the infrastructure conditions, the amount of waste or product to be processed locally, and the specific energy needs to be covered.

NOMENCLATURE

BMP: Biochemical methane potential

BPW: Banana peel waste

BPW-C: Banana peel waste carbon

CE: Coulombic efficiency

CV: Cycling voltammetry

d.b.: Dry basis

DFT: Density functional theory

EB: Energy balance

ESS: Energy storage systems

GAL: Lactic acid, sodium acetate and glucose solution

MS: Total mineral solids (%)

NLDFT: Non-local density functional theory

NMP: 1-methyl-2-pyrrolidinone

PVDF: Polyvinylidene fluoride

SEI: Solid electrolyte interphase

STP: Standard temperature and pressure (0ºC, 1 at

S_{BET}: Brunauer-Emmett-Teller surface area (m^2/g)

TC: Soluble total carbon (mg/kg)

TGA: Thermogravimetric analysis

TOC: Soluble total organic carbon (mg/kg)

G_T: Maximum methane volume produced (mL)

HCV: Higher calorific value (kcal/kg)

IC: Soluble inorganic carbon (mg/kg)

LCV: Lower calorific value (kcal/kg)

LIB: Lithium-ion battery

TS: Total solids (%)

TSN: Total soluble nitrogen (mg/L)

VS: Total volatile solids (%)

XRD: X-Ray Diffraction

Acknowledgements

The authors are very grateful to the Ministry of Economy, Industry and Competitiveness (Project MAT2017-87541-R), Junta de Andalucía (Group FQM-175) and Asociación Universitaria Iberoamericana de Postgrado, for funding this research study.

References

[1] Z. Anwar, M. Gulfraz, M.Irshad. Agro-industrial lignocellulosic biomass a key to unlock the future bio-energy: A brief review. Journal of Radiation Research and Applied Sciences, 7(2), 2014: 163-173.

[2] FAO, FAOSTAT, (2018). http://www.fao.org/faostat/es/#data/QC (accessed August 18, 2020).

[3] F.F. Vidal, P.E. Pereira, M.D.O.R. Vázquez, P.J. Sotolongo, J.Y. Quintana, A. Ortiz, Efecto de la suplementación con pseudotallo de plátano sobre la salud y el peso al sacrificio de cerdos comerciales, Rev. Prod. Anim. 13 (2001).

[4] B.B.C. Canto, G.M.A. Castillo, Un mil usos: el plátano, Revista de Divulgación Científica y Tecnológica de La Universidad Veracruzana. 24 (2011) 1–3.

[5] L.G. Blasco, M.F. Gómez, Propiedades funcionales del plátano (Musa sp), Revista Médica Universidad Veracruzana. 1 (2014) 22–26.

[6] A. Mohiuddin, M.K. Saha, M.S. Hossian, A. Ferdoushi, Usefulness of Banana (*Musa paradisiaca*) Wastes in Manufacturing of Bio-products: A Review, The Agriculturists. (2014).

[7] R. Gumisiriza, J.F. Hawumba, M. Okure, O. Hensel, Biomass waste-to-energy valorisation technologies: A review case for banana processing in Uganda, Biotechnology for Biofuels. (2017).

[8] B.D. Hennig, In Focus: The unchanging politics of climate change, Political Insight. 10 (2019) 20–21.

[9] K. Ku Ahmad, K. Sazali, A.A. Kamarolzaman, Characterisation of fuel briquettes from banana tree waste, in: Materials Today: Proceedings, 2018. https://doi.org/10.1016/j.matpr.2018.07.027.

[10] A.F. Rojas, S. Rodríguez-Barona, J. Montoya. Evaluación de alternativas de aprovechamiento energético y bioactivo de la cáscara de plátano. Información Tecnológica, 30(5), 11-24. 2019.

[11] M. H. Tahir, Z. Zhao, J. Ren, T. Rasool, S.R. Naqvi. Thermo-kinetics and gaseous product analysis of banana peel pyrolysis for its bioenergy potential. Biomass and Bioenergy 122 (2019) 193-201.
[12] F.G.D. Thulu, O. Kachaje, T. Mlowa. 2016. A study of combustion characteristics of fuel briquettes from a blend of banana peelings and saw dust in Malawi. International Journal of Thesis Projects and Dissertations (IJTPD), 4(3): 135-158.
[13] M.N. Acda. Physical and chemical properties of fuel pellets from agricultural residues. Philippine Agricultural Scientist, 99(3): 283-287.
[14] Elviana, OSL Toding, C. Virginia S. Suhartini (2018). Conversion banana and orange peel into electricity using microbial fuel cell. IOP Conf. Series: Earth and Environmental Science 209, 012049.
[15] P.K. de Souza, R Battisti, O. Souza, N. Sellin, R.A.F., Machado, C. Marangoni. Integration of banana crop residues as biomass feedstock into conventional production of fist-generation fuel ethanol from sugarcane: a simulation-based case study. Biofuels, Bioproducts and Biorefining, 15(3):671-689.
[16] N. Pisutpaisal, S. Boonyawanich, H. Saowaluck, Feasibility of biomethane production from banana peel, Energy Procedia. 50 (2014) 782–788.
[17] M.O. Jesuyemi, B. Charnnok, K. Saritpongteeraka, S. Chaiprapat, M.J. Odedina, B. Charnnok, K. Saritpongteeraka, S. Chaiprapat, Effects of size and thermophilic pre-hydrolysis of banana peel during anaerobic digestion, and biomethanation potential of key tropical fruit wastes, Waste Management. 68 (2017) 128–138.
[18] N. Tripathi, C.D. Hills, R.S. Singh, C.J. Atkinson, Biomass waste utilisation in low-carbon products: harnessing a major potential resource, Npj Climate and Atmospheric Science. (2019).
[19] C. Jin, J. Nai, O. Sheng, H. Yuan, W. Zhang, X. Tao, X.W. Lou, Biomass-based materials for green lithium secondary batteries, Energy and Environmental Science. (2021) 14, 1326-1379.
[20] J. Wang, P. Nie, B. Ding, S. Dong, X. Hao, H. Dou, X. Zhang, Biomass-derived carbon for energy storage devices, Journal of Materials Chemistry A. (2017).
[21] O. Fromm, A. Heckmann, U.C. Rodehorst, J. Frerichs, D. Becker, M. Winter, T. Placke, Carbons from biomass precursors as anode materials for lithium-ion batteries: New insights into carbonisation and graphitisation behavior and into their correlation to electrochemical performance, Carbon. (2018).
[22] L. Fan, L. Fan, T. Yu, X. Tan, Z. Shi, Hydrothermal synthesis of lignin-based carbon microspheres as anode material for lithium-ion batteries, International Journal of Electrochemical Science. 15 (2020) 1035–1043.
[23] Z. Wu, L. Wang, J. Huang, J. Zou, S. Chen, H. Cheng, C. Jiang, P. Gao, X. Niu, Loofah-derived carbon as an anode material for potassium ion and lithium-ion batteries, Electrochimica Acta. (2019).
[24] P. Salimi, S. Javadian, O. Norouzi, H. Gharibi, Turning an environmental problem into an opportunity: potential use of biochar derived from a harmful marine biomass named Cladophora glomerata as anode electrode for Li-ion batteries, Environmental Science and Pollution Research. (2017).
[25] X. Zhang, Y. Li, D. Li, J. Xiao, W. Zhang, Y. Xu, Rice husk derived porous carbon decorated with hierarchical molybdenum disulfide microflowers: Synergistic lithium storage performance and lithiation kinetics, International Journal of Hydrogen Energy. 44 (2019) 7438–7447.

[26] L. Jiang, L. Sheng, Z. Fan, Biomass-derived carbon materials with structural diversities and their applications in energy storage, Science China Materials. (2018).
[27] A. Caballero, L. Hernán, J. Morales, Limitations of disordered carbons obtained from biomass as anodes for real lithium-ion batteries, ChemSusChem. (2011).
[28] Stephan, A.M., Kumar, T.P., Ramesh, R., Thomas, S., Jeong, S.K., Nahm, K.S. (2006). Pyrolitic carbon from biomass precursors as anode materials for lithium batteries. Material Science and Engineering: A. 430 (1-2): 132-137.
[29] J.A. Siles, F. Vargas, M.C. Gutiérrez, A.F. Chica, M.A. Martín, Integral valorisation of waste orange peel using combustion, biomethanisation and co-composting technologies, Bioresource Technology. (2016).
[30] Royal Decree 687/2011 of 13 May, which amends Royal Decree 430/2004 of 12 March establishing new rules on the limitation of emissions into the atmosphere of certain pollutants from large combustion plants, and fixing certain conditions for the control of emissions into the atmosphere of oil refineries. Boletín Oficial del Estado, 2011, 125, 52177.
[31] D.R. Lide, ed., Handbook of Chemistry and Physics, 85th ed., CRC Press, London, New York, Washington, D.C., 2004.
[32] US Council Composting, Test methods for the examination of composting and compost, 2001.
[33] APHA, Standard Methods for Examination of Water and Wastewater, 17th 6 ed, Association, American Public Health, Washington, DC, 1989.
[34] N. Scarlat, V. Motola, J.F. Dallemand, F. Monforti-Ferrario, L. Mofor, Evaluation of energy potential of Municipal Solid Waste from African urban areas, Renewable and Sustainable Energy Reviews. (2015).
[35] A. Chambers, Renewable energy in non-technical language, PennWell Books, Houston, 2003.
[36] Ministerio de Ambiente Vivienda y Desarrollo Territorial- República de Colombia, Resolución 909, 2008.
[37] N. De Nevers, Air pollution control engineering, Waveland Press, Incorporated, 2017.
[38] M.B.G. De Oliveira, O. Souza, C. Marangoni, D. Hotza, A.P.N. De Oliveira, N. Sellin, Production and characterisation of fuel briquettes from banana leaves waste, Chemical Engineering Transactions. (2014). https://doi.org/10.3303/CET1437074.
[39] K.F. Fannin, Start-up, operation, stability, and control., Elsevier Applied Science, London, UK, 1987.
[40] A. Wheatley, Anaerobic digestion : a waste treatment technology, Elsevier Applied Science, London, 1990.
[41] R.F. Hickey, S. Goodwin, Anaerobic processes, Journal Water Pollution Control Federation. 61 (1989) 814–821.
[42] S. Goodwin, R.F. Hickey, Anaerobic processes, Journal Water Pollution Control Federation. 60 (1988) 831–837.
[43] D.T. Hill, S.A. Cobb, J.P. Bolte, Using volatile fatty acid relationships to predict anaerobic digester failure, Transactions of the American Society of Agricultural Engineers. (1987).
[44] N. Bardiya, D. Somayaji, S. Khanna, Biomethanation of banana peel and pineapple waste, Bioresource Technology. 58 (1996) 73–76. https://doi.org/10.1016/S0960-8524(96)00107-1.
[45] M.O. Jesuyemi, B. Charnnok, K. Saritpongteeraka, S. Chaiprapat, Effects of size and thermophilic pre-hydrolysis of banana peel during anaerobic digestion, and

biomethanation potential of key tropical fruit wastes, Waste Management. 68 (2017) 128–138.
[46] Y. Joute, E. Bari, S. Belhadj, F. Karouach, Y. Gradi, W. Stelte, A.B. Bjerre, SEMI-CONTINUOUS ANAEROBIC CO-DIGESTION OF COW MANURE AND BANANA WASTE: EFFECTS OF MIXTURE RATIO, Applied Ecology and Environmental Research. 14 (2016) 337–349.
[47] V.B. Barua, V. Rathore, A.S. Kalamdhad, Anaerobic co-digestion of water hyacinth and banana peels with and without thermal pretreatment, Renewable Energy. 134 (2019) 103–112.
[48] Angelidaki, B.K. Ahring. 1994. Anaerobic thermophilic digestion of manure at different ammonia loads: effect of temperature. Water Res., 28 (1994), pp. 727-731
[49] Y. Chen, J.J. Cheng, K.S. Creamer, Inhibition of anaerobic digestion process: A review, Bioresource Technology. (2008).
[50] F.S. al Amri, M.A. Hossain, Comparison of total phenols, flavonoids and antioxidant potential of local and imported ripe bananas, Egyptian Journal of Basic and Applied Sciences. (2018).
[51] R.C. da S. Mazareli, A.C. Villa Montoya, T.P. Delforno, V.B. Centurion, V.M. de Oliveira, E.L. Silva, M.B.A. Varesche, Enzymatic routes to hydrogen and organic acids production from banana waste fermentation by autochthonous bacteria: Optimisation of pH and temperature, International Journal of Hydrogen Energy. 46 (2021) 8454–8468.
[52] A. Koppar, P. Pullammanappallil, Anaerobic digestion of peel waste and wastewater for on-site energy generation in a citrus processing facility, energy. 60 (2013) 62–68.
[53] J.Y. Tock, C.L. Lai, K.T. Lee, K.T. Tan, S. Bhatia, Banana biomass as potential renewable energy resource: A Malaysian case study, Renewable and Sustainable Energy Reviews. (2010).
[54] A. Gil, J.A. Siles, A. Serrano, A.F. Chica, M.A. Martín, Effect of variation in the C/[N+P] ratio on anaerobic digestion, Environmental Progress & Sustainable Energy. 38 (2019) 228–236.
[55] S. Aiyuk, I. Forrez, D.K. Lieven, A. van Haandel, W. Verstraete. Anaerobic and complementary treatment of domestic sewage in regions with hot climates—a review. Bioresour. Technol., 97 (2006), pp. 2225-2241
[56] A. Hoque, A. Clarke, Greening of industries in Bangladesh: Pollution prevention practices, Journal of Cleaner Production. 51 (2013) 47–56.
[57] J.C. Arrebola, A. Caballero, L. Hernán, J. Morales, M. Olivares-Marín, V. Gómez-Serrano, Improving the performance of biomass-derived carbons in Li-Ion batteries by controlling the lithium insertion process, Journal of The Electrochemical Society. (2010).
[58] H. Song, N. Li, H. Cui, C. Wang, Enhanced storage capability and kinetic processes by pores- and hetero-atoms- riched carbon nanobubbles for lithium-ion and sodium-ion batteries anodes, Nano Energy. 4 (2014) 81–87.
[59] C. Choi, S.D. Seo, B.K. Kim, D.W. Kim, Enhanced Lithium storage in hierarchically porous carbon derived from waste tea leaves, Scientific Reports. (2016). https://doi.org/10.1038/srep39099.
[60] J. Ma, F. Yu, Z. Wen, M. Yang, H. Zhou, C. Li, L. Jin, L. Zhou, L. Chen, Z. Yuan, J. Chen, A facile one-pot method for synthesis of low-cost iron oxide/activated carbon nanotube electrode materials for lithium-ion batteries, Dalton Transactions. 42 (2013) 1356–1359.

[61] Z. Nie, Y. Huang, B. Ma, X. Qiu, N. Zhang, X. Xie, Z. Wu, Nitrogen-doped carbon with modulated surface chemistry and porous structure by a stepwise biomass activation process towards enhanced electrochemical Lithium-Ion storage, Scientific Reports. (2019). https://doi.org/10.1038/s41598-019-50330-w.
[62] E. Duraisamy, A. Prasath, V. Sankar Devi, M.N.M. Ansari, P. Elumalai, Sustainably-derived hierarchical porous carbon from spent honeycomb for high-performance lithium-ion battery and ultracapacitors, Energy Storage. (2020).
[63] J.H. Um, C.Y. Ahn, J. Kim, M. Jeong, Y.E. Sung, Y.H. Cho, S.S. Kim, W.S. Yoon, From grass to battery anode: Agricultural biomass hemp-derived carbon for lithium storage, RSC Advances. (2018).
[64] F. Luna-Lama, D. Rodríguez-Padrón, A.R. Puente-Santiago, M.J. Muñoz-Batista, A. Caballero, A.M. Balu, A.A. Romero, R. Luque, Non-porous carbonaceous materials derived from coffee waste grounds as highly sustainable anodes for lithium-ion batteries, Journal of Cleaner Production. (2019).
[65] A.K. Mondal, K. Kretschmer, Y. Zhao, H. Liu, H. Fan, G. Wang, Naturally nitrogen-doped porous carbon derived from waste shrimp shells for high-performance lithium-ion batteries and supercapacitors, Microporous and Mesoporous Materials. (2017).
[66] S. Sekar, Y. Lee, D.Y. Kim, S. Lee, Substantial LIB anode performance of graphitic carbon nanoflakes derived from biomass green-tea waste, Nanomaterials. (2019).
[67] H. Ru, K. Xiang, W. Zhou, Y. Zhu, X.S. Zhao, H. Chen, Bean-dreg-derived carbon materials used as superior anode material for lithium-ion batteries, Electrochimica Acta. 222 (2016) 551–560.
[68] Z. Guan, Z. Guan, Z. Li, J. Liu, K. Yu, Characterisation and preparation of nanoporous carbon derived from hemp stems as anode for Lithium-Ion batteries, Nanoscale Research Letters. (2019).
[69] C. Hernández-Rentero, V. Marangon, M. Olivares-Marín, V. Gómez-Serrano, Á. Caballero, J. Morales, J. Hassoun, Alternative lithium-ion battery using biomass-derived carbons as environmentally sustainable anode, Journal of Colloid and Interface Science. (2020).
[70] Kaifeng. Yu, Jian. Li, Hui. Qi, Ce. Liang, Cellulose-derived hollow carbonaceous nanospheres from rice husks as anode for Lithium-Ion batteries with enhanced reversible capacity and cyclic performance, ChemistrySelect. 2 (2017).

Figure captions

Figure 1. A) Variation in pH in the mixing liquor of the digesters with the load added. B) Variation in the concentration of individual volatile organic acids (acetic, propionic, isobutyric and isovaleric) with the load added to the anaerobic digesters. C) Experimental maximum methane volume produced against the load added to the reactors.

Figure 2. Evolution of the concentration of total soluble nitrogen (A) and soluble phosphorus (B) with the organic load.

Figure 3. A) XRD diffractogram. B) TGA curves recorded in N_2 and O_2 atmospheres. C) Nitrogen adsorption-desorption isotherm. D) DFT pore size distribution of BPW-C activated carbon.

Figure 4. A) CV curves recorded at 0.1 mV/s of BPW-C electrode. B) Charge-discharge galvanostatic profiles at 0.2 C (74.4 mA/g) of BP-C electrode.

Figure 5. A) Charge-discharge profiles at different current rates of BPW-C electrode. B) Variation in the specific capacity with the current rate for different biomass carbons reported from literature.

Figure 1.

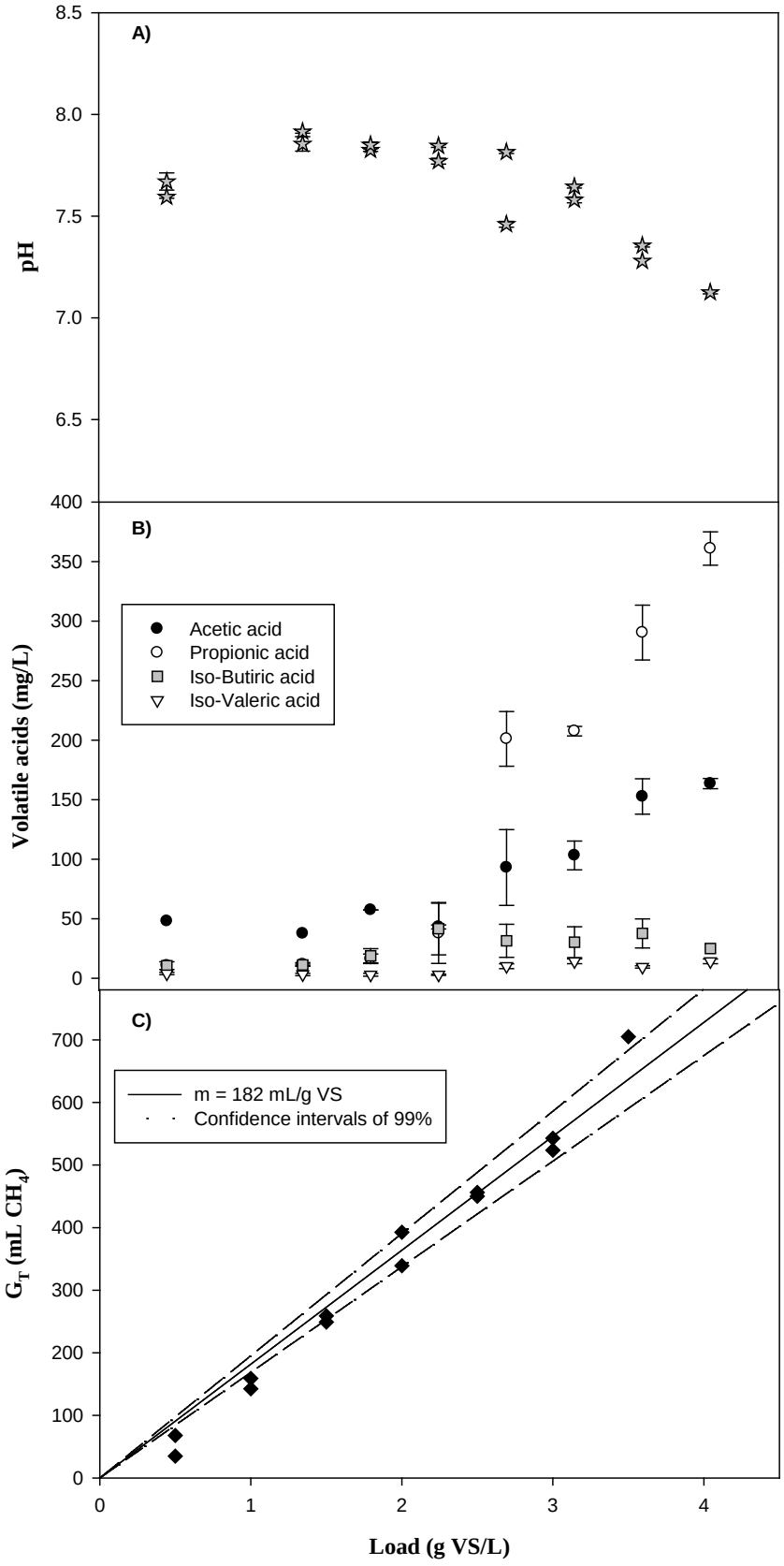
A)
pH
8.5
8.0
7.5
7.0
6.5
B)
Volatile acids (mg/L)
400
350
300
250
200
150
100
50
0
Acetic acid
Propionic acid
Iso-Butiric acid
Iso-Valeric acid
C)
G_T (mL CH_4)
700
600
500
400
300
200
100
0
m = 182 mL/g VS
Confidence intervals of 99%
0
1
2
3
4
Load (g VS/L)

Figure 2.

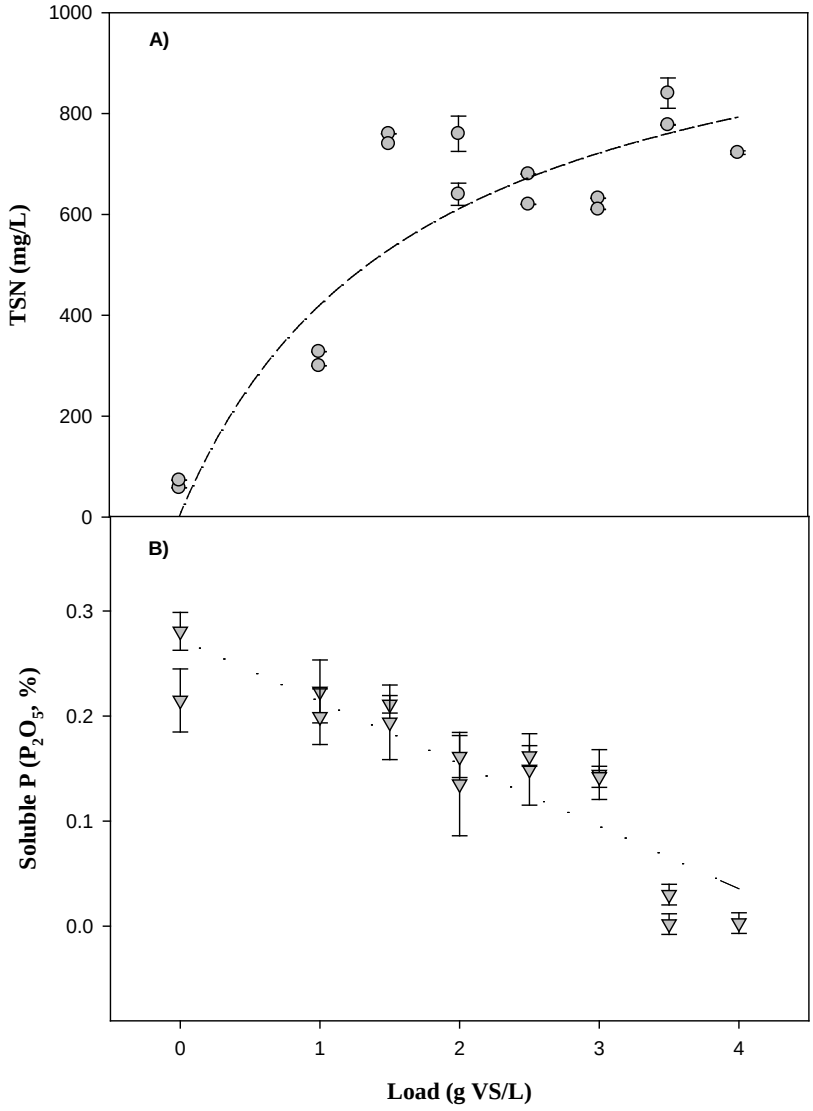
A)
B)
TSN (mg/L)
Soluble P (P_2O_5, %)
Load (g VS/L)
1000
800
600
400
200
0
0.3
0.2
0.1
0.0
0
1
2
3
4

Figure 3.

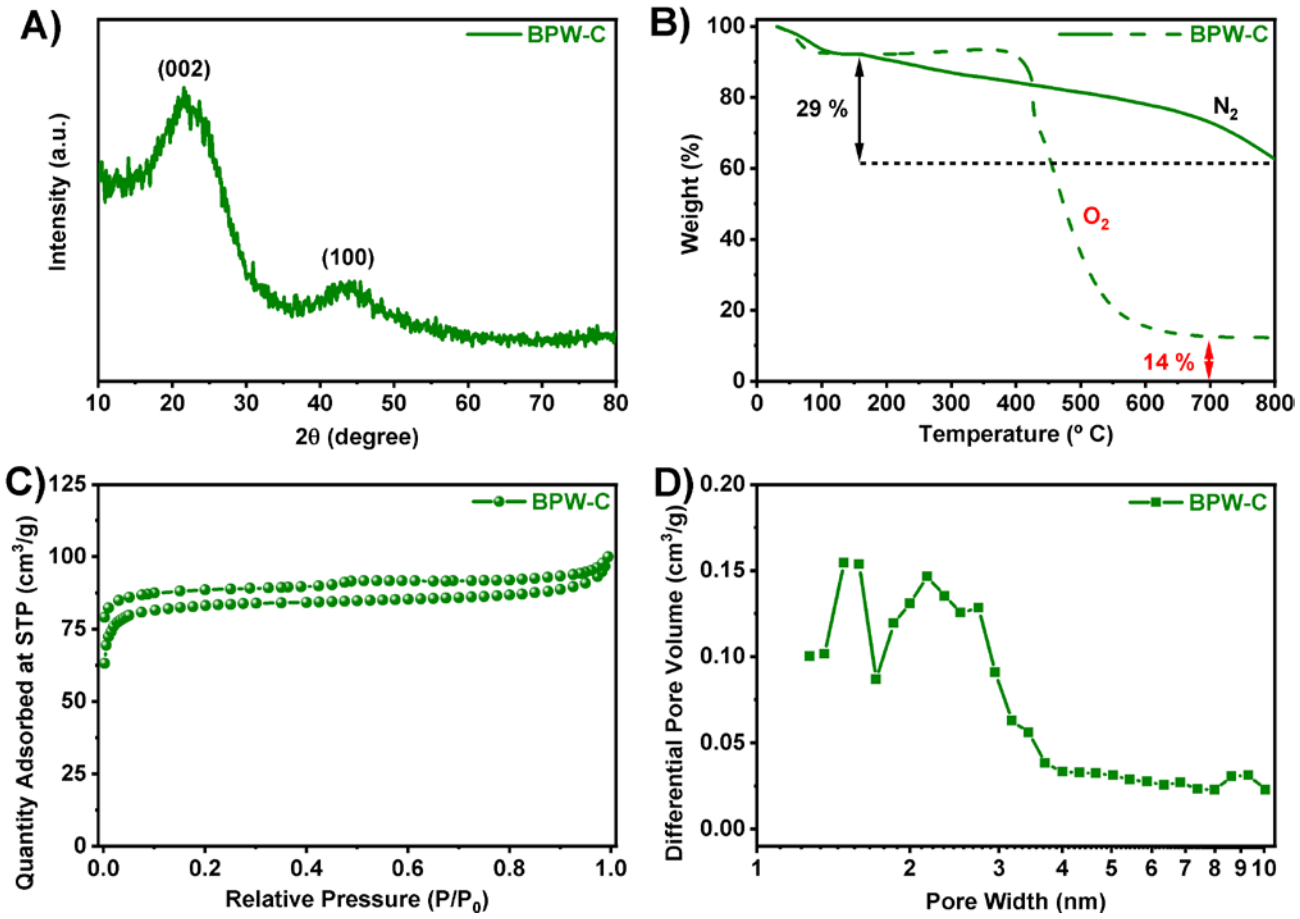
A)
BPW-C
(002)
(100)
Intensity (a.u.)
2θ (degree)
B)
BPW-C
29 %
N2
O2
14 %
Weight (%)
Temperature (° C)
C)
BPW-C
Quantity Adsorbed at STP (cm3/g)
Relative Pressure (P/P0)
D)
BPW-C
Differential Pore Volume (cm3/g)
Pore Width (nm)

Figure 4.

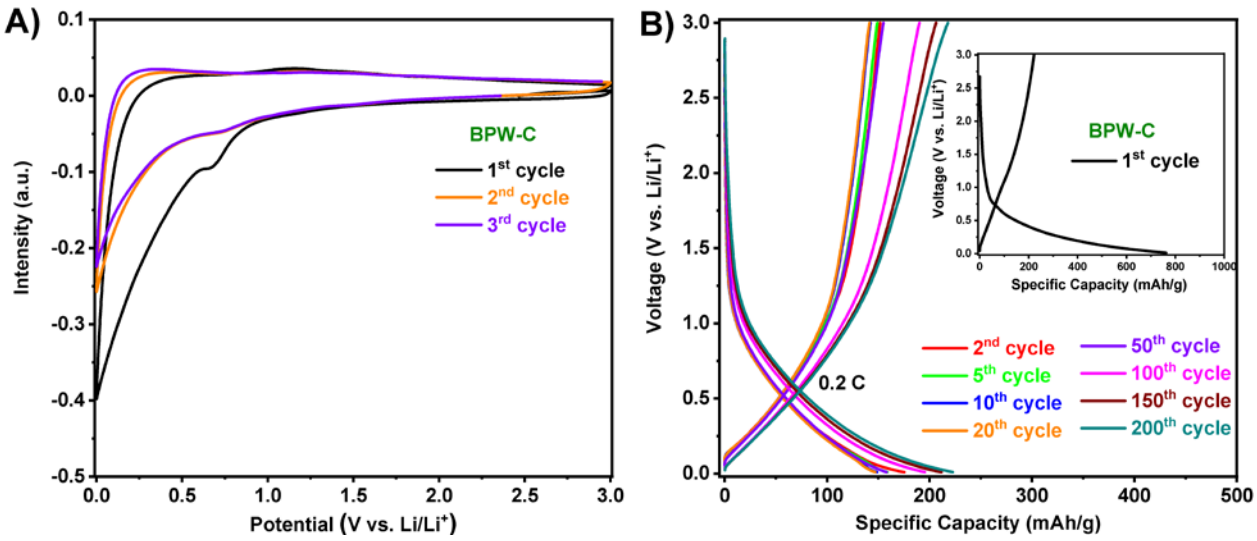
A)
Intensity (a.u.)
Potential (V vs. Li/Li+)
BPW-C
1st cycle
2nd cycle
3rd cycle
B)
Voltage (V vs. Li/Li+)
Specific Capacity (mAh/g)
0.2 C
2nd cycle
5th cycle
10th cycle
20th cycle
50th cycle
100th cycle
150th cycle
200th cycle
BPW-C
1st cycle

Figure 5.

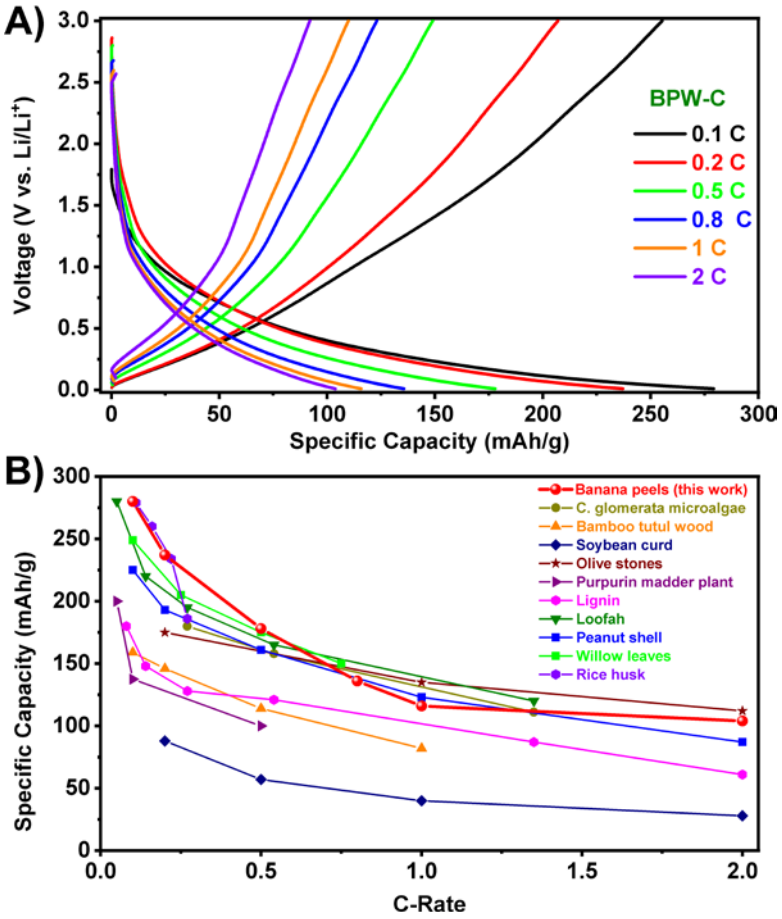
A)
Voltage (V vs. Li/Li+)
Specific Capacity (mAh/g)
BPW-C
0.1 C
0.2 C
0.5 C
0.8 C
1 C
2 C
B)
Specific Capacity (mAh/g)
C-Rate
Banana peels (this work)
C. glomerata microalgae
Bamboo tutul wood
Soybean curd
Olive stones
Purpurin madder plant
Lignin
Loofah
Peanut shell
Willow leaves
Rice husk

Table 1. Chemical composition of BPW and BPW-C (in dry basis).

BPW	
Parameter	Mean value ± Standard deviation
Conductivity (µs/cm)	4392 ± 0.02
pH	4.21 ± 0.04
Moisture (%)	89.09 ± 0.09
P_2O_5 (%)	0.16 ± 0.05
TC (mg/kg)	2254 ± 1
IC (mg/kg)	62 ± 1
TOC (mg/kg)	2192 ± 1
TS (%)	10.91 ± 0.09
MS (%)	1.17 ± 0.01
VS (%)	9.74 ± 0.08
Acetic acid (mg/kg)	135 ± 5
Propionic acid (mg/kg)	8 ± 1
Isobutiric acid (mg/kg)	57 ± 3
Butiric acid (mg/kg)	< 1
Isovaleric acid (mg/kg)	< 1
Valeric acid (mg/kg)	< 1
Cu (mg/kg)	6.5 ± 0.3
Cr (mg/kg)	0.7 ± 0.9
Ni (mg/kg)	13.6 ± 0.3
Cd (mg/kg)	5.5 ± 0.3
Pb (mg/kg)	14.2 ± 2.6
Zn (mg/kg)	24.5 ± 5.4
C (%)[a]	43.71 ± 0.07
H (%)[a]	5.66 ± 0.50
N (%)[a]	1.46 ± 0.08
O (%)[a]	40.87 ± 0.9
S (%)[a]	0.07 ± 0.01

BPW-C				
C (%)[a]	N (%)[a]	S_{BET} (m^2/g)	V_{total} (cm^3/g)	Pore size (nm)
83.15	1.19	264	0.155	2.39

a: (% w/w)